

Supplemental Methods

Electrophoresis and Western Blotting

Protein extracts were adjusted to contain 30% glycerol, 2% SDS, 62.5 mM Tris, 0.02% bromophenol blue, and 10% β -mercaptoethanol. Approximately 30 μ g of protein per sample was then loaded on a 4-12% bis-tris Nupage (Invitrogen, Carlsbad, CA) or 10% polyacrylamide gel and electrophoresed for 30 minutes at 100 V followed by 200 V for 45 minutes to 1 hour. The separated proteins were transferred to a PVDF membrane (Immobilon-P, Millipore, Bedford, MA) by blotting at 200 V for 2 hours at RT in Nupage Transfer buffer with 20% methanol (Invitrogen, Carlsbad, CA). The blot was blocked for 1 hour at RT in 5% bovine serum albumin (BSA) in phosphate buffered saline plus 0.1 % Tween-20 (PBST) and incubated overnight at 4 °C in the appropriate dilution of the primary antibody: 1:500 anti-PC rabbit polyclonal antibody (Santa Cruz Biotechnology, Santa Cruz, CA), 1:1000 or 1:2000 anti-GLS1 mouse monoclonal antibody (Abcam, Cambridge, MA or Abnova, Taipei City, Taiwan), and 1:50000 anti- α -tubulin rabbit monoclonal antibody (Epitomics, Burlingame, CA). After rinsing, the membranes were incubated for 1 hour at RT in a 1:2000 dilution of the appropriate secondary antibody, horseradish peroxidase (HRP) conjugated goat anti-mouse or anti-rabbit IgG (Pierce-Rockford, IL). Finally, after incubation with chemoluminescent HRP substrate (Supersignal West Dura Extended Duration Substrate, Thermo Fisher Scientific, Rockford, IL), the membranes were exposed to X-Ray film for an appropriate time. The films were digitized using a high-resolution scanner and band intensities were measured using Quantity One software (Bio-Rad, Hercules, CA). PC and GLS1 band intensities were normalized to that of α -tubulin.

Immunohistochemistry

To determine the spatial distribution of PC in lung tissues, immunohistochemistry was performed on tissue sections obtained from nine patients diagnosed with NSCLC. All steps were performed on a Leica Bond III (Leica Microsystems Ltd, Newcastle Upon Tyne, UK) and unless otherwise stated, all reagents were obtained from Leica Microsystems. Dewaxing was performed at 72 °C in Bond TM Dewax Solution, followed by washing with ethanol and Bond TM Wash Solution. Epitope retrieval was performed at 100 °C for 20 min with Bond TM Epitope Retrieval Solution 2. The sections were then washed again with Bond TM Wash Solution. The sections were blocked, first by treatment with 3% hydrogen peroxide for five minutes and then washed three times in Bond TM Wash Solution. The slides were then incubated for 15 min in a 1:50 dilution anti-PC antibody (Santa Cruz Biotechnology, Santa Cruz, CA). After rinsing with Bond TM Wash Solution, the slides were incubated in Bond TM Polymer Refine Detection for 8 min at RT, and rinsed again with Bond TM Wash Solution and distilled water and incubated for 10 min with Mixed DAB Refine for 10 min. Finally, after three washes with distilled water, the sections were counterstained with hematoxylin for 5 min.

Cell proliferation assay

Transduced cells (3000 cells/well) were seeded onto 96-well plates. Every 24 hours, the media was refreshed. To assess cell density, cells were washed in PBS, fixed in 50% ethanol, incubated in 0.2% Janus Green reagent and extracted in 0.5 M HCl before absorbance at 610 nm was measured as described (1).

Colony formation assay

At the stated number of days post transduction, 60,000 cells transduced with either shEV, shPC54, or shPC55 were seeded in 1 mL 0.03% agarose, above a 1 mL layer of 0.05% agarose in a 6 well plate. 1 mL fresh media was added once a week and colony formation was assessed visually after staining in violet crystal under a microscope.

Fluorescence microscopy

Cells were seeded on coverslips in 6-well plates. After 48 hours, cells were fixed in 4%

paraformaldehyde and permeabilized with 0.1% Triton X-100. Nuclei, actin filaments, and mitochondria were stained respectively with Hoechst 33342, Alexa 488 conjugated to phalloidin, and MitoTracker® Red CMXRos (Invitrogen, Eugene, OR). Alternatively, PC was stained by incubation in a 1:50 dilution of anti-PCB rabbit monoclonal antibody (Santa Cruz Biotechnology) followed by incubation with Alexa 488 conjugated to anti-rabbit antibody (Invitrogen, Eugene, OR).

GLS1 knockdown

GLS1 knockdown was performed in the same manner as described for PC knockdown in Methods and using Mission® shRNA from Sigma. The sequences used for GLS1 knockdown were:
shGLS36: CCGGGCCCTGAAGCAGTTCGAAATACTCGAGTATTTTCTGAACTGCTTCAGGGGCTTTTTTG
shGLS37: CCGGGATGGTGTTCATGCTAGACAAACTCGAGTTTGTCTAGCATGACACCATCTTTTTG

FT-ICR-MS analysis of lipids and nucleotides in Fig. S13

The polar and non-polar metabolite extracts were prepared from A549 cells as described in Methods. Both extracts were analyzed by continuous infusion into a 7 T Qh/FT-ICR hybrid MS (Solarix XR, Bruker, Billerica, MA, USA) equipped with a Triversa Nanomate nanoESI ion source (Advion Biosciences, Ithaca, NY).

The polar fraction was removed of matrix ions using C18 Tips (Thermo Scientific Pierce, Rockford, IL) as described previously (2). The cleaned up polar fraction containing the nucleotides was diluted 1:10 in isopropanol:methanol:chloroform (4:2:1) for FT-ICR-MS analysis in the negative ion mode. The instrument was calibrated using a standard mix of nucleotides before acquisition. The Triversa Nanomate was operated at 1.3 kV and 0.3 psi head pressure using the “A” chip (5.5 µm nozzle), which yielded stable spray for more than 15 minutes. The mass spectra was acquired in the mass range of 250 m/z – 800 m/z with a target mass resolution of 1,100,000 at 400 m/z. Ion accumulation time was set to 0.025 s resulting in a total ion count between 1×10^8 - 3×10^8 per scan. 100 such scans were added to give the final spectra. The total run time per sample was 13 minutes.

Non-polar fractions were analyzed for lipids by 1:20 dilution in isopropanol:methanol:chloroform (4:2:1) plus 5 mM ammonium formate. Data was acquired in the positive ion mode. The instrument was calibrated using ESI Tune Mix (Fluka, Sigma-Aldrich, St.Louis, MO) before acquisition. The Nanomate was operated at 1.5 kV and 0.4 psi head pressure using the “A” chip (5.5 µm nozzle). The mass spectra was acquired in the mass range of 150 m/z – 3000 m/z with a target mass resolution of 790,000 at 400 m/z. Ion accumulation time was set to 0.015s resulting in a total ion count between 1×10^8 - 3×10^8 per scan. 100 scans were added to give the final spectra. The total run time per sample was 13 minutes.

The data obtained were exported as an Excel file and processed as described previously (2, 3).

References

1. Raspotnig G, Fauler G, Jantscher A, Windischhofer W, Schachl K, and Lei H. Colorimetric Determination of Cell Numbers by Janus Green Staining. *Analytical Biochemistry*. 1999;275 74-83.
2. Lorkiewicz PK, Higashi RM, Lane AN, and Fan TW-M. High information throughput analysis of nucleotides and their isotopically enriched isotopologues by direct-infusion FTICR-MS. *Metabolomics*. 2012;8 930-9
3. Lane AN, Fan TW-M, Xie X, Moseley HN, and Higashi RM. Stable isotope analysis of lipid

Supplemental Tables

Table S1: Statistical distributions for PC and GLS1 expression in human lung

Parameter	PC			GLS1		
	CA	NC	CA/NC	CA	NC	CA/NC
Mean	0.620	0.157	75	0.40	0.807	10.15
Sd	0.73	.039	241.2	0.57	1.86	31.1
Median	0.435	0.045	6.71	0.173	0.237	0.797
Mode*	0.075	0.01	3.2	<0.1	<0.1	0.6

Expression was determined by Western blot analysis of 86 paired samples (n=172) of resected human NSCLC and the adjacent benign lung tissue with normalization to α -tubulin. The expression values vary widely among individuals, and are non-normally distributed, as shown by the comparison of the mean, median and estimated modal values. Significance was therefore tested using the non-parametric Wilcoxon test for paired samples. *Mode was estimated from histograms, and thus is somewhat dependent on the bin size.

Wilcoxon p value PC CA versus NC: <0.0001

Wilcoxon p value GLS1 CA versus NC p=0.213

Table S2: Patient plasma glucose concentrations and enrichment

		Average	Std Error
Post Infusion	¹² C Glc (mM)	3.24	0.08
	¹³ C Glc (mM)	2.83	0.2
	Percent Enrichment	44%	2%
Post OR	¹² C Glc (mM)	3.59	0.1
	¹³ C Glc (mM)	0.742	0.06
	Percent Enrichment	17%	1%
Δ	¹³ C Glc (mM)	2.09	0.2
	Percent Enrichment	27%	2%

Human NSCLC patients were given a bolus injection of 10 g ¹³C₆-glucose as described in Methods. The blood of 65 patients was taken immediately after the infusion of glucose (post infusion) and after tumor resection (post OR). The concentrations of unlabeled (¹²C Glc) and labeled (¹³C Glc) glucose were measured by ¹H NMR. Percent enrichment was calculated by dividing the concentration of ¹³C labeled glucose (¹³C Glc) by the concentration of total glucose (¹³C Glc + ¹²C Glc). Changes in the concentration and enrichment of the labeled glucose as it was cleared from the blood stream from the time of infusion to the time of tumor resection were also calculated (Δ).

Table S3: Mouse xenograft growth rate parameters and statistics

	shEV	shPC
a (mm ²)	13.98±1.7	13.82±1.6
b (mm ² /d ²)	0.076±0.003	0.041±0.003
χ^2	51.3	40.8
R ²	0.989	0.969

Six each 6-week-old female NOD/SCID gamma (NSG) mice were injected with A549 cells containing either shEV or shPC55 and the resulting tumor sizes were measured as described in Methods. Growth curves were fitted by non-linear regression to a simple quadratic where size= $a+bt^2$. In this form, a is the initial tumor size at t=0, and b is the specific growth rate. The standard deviations were derived from the covariance matrix and the residual chi² (χ^2). Comparing the specific growth rate b for cancer and non-cancer gave P<0.0001 for N=6 mice per group and eight time points.

Supplemental Figures

Figure S1: Human NSCLC tumors have enhanced glucose oxidation through glycolysis and the Krebs cycle compared to paired non-cancerous lung tissues

A: Human patients were infused with $^{13}\text{C}_6$ -glucose prior to having their NSCLC tumor resected. The cancer tissues contained significantly more labeled lactate and less labeled glucose compared to paired benign tissue from the same patient. Labeled concentrations were calculated from the H3 peak of lactate and the anomeric proton of α -glucose from the $^1\text{H}\{^{13}\text{C}\}$ HSQC NMR spectra of 27 patients.

B: Fractional enrichment of Krebs cycle intermediates citrate (Cit), glutamate (Glu), succinate (Succ), fumarate (Fum), malate (Mal), and aspartate (Asp) from the cancerous and non-cancerous lung of 34 patients as determined by GCMS reveal an enhanced production of m+2 or $^{13}\text{C}_2$ isotopologues. This suggests elevated glucose oxidation via PDH in cancerous tissues. The diagram shows how PDH can produce the m+2

isotopologues from the $^{13}\text{C}_3$ -pyruvate derived from glycolysis.

C: The full isotopologue distribution for Krebs cycle metabolites, as measured by GCMS (N=34).

*, p<0.05, ** :p<0.01, ***:p<0.001, ****:p<0.0001 according to the Student t-Test assuming unequal variances; Error bars represent the standard error.

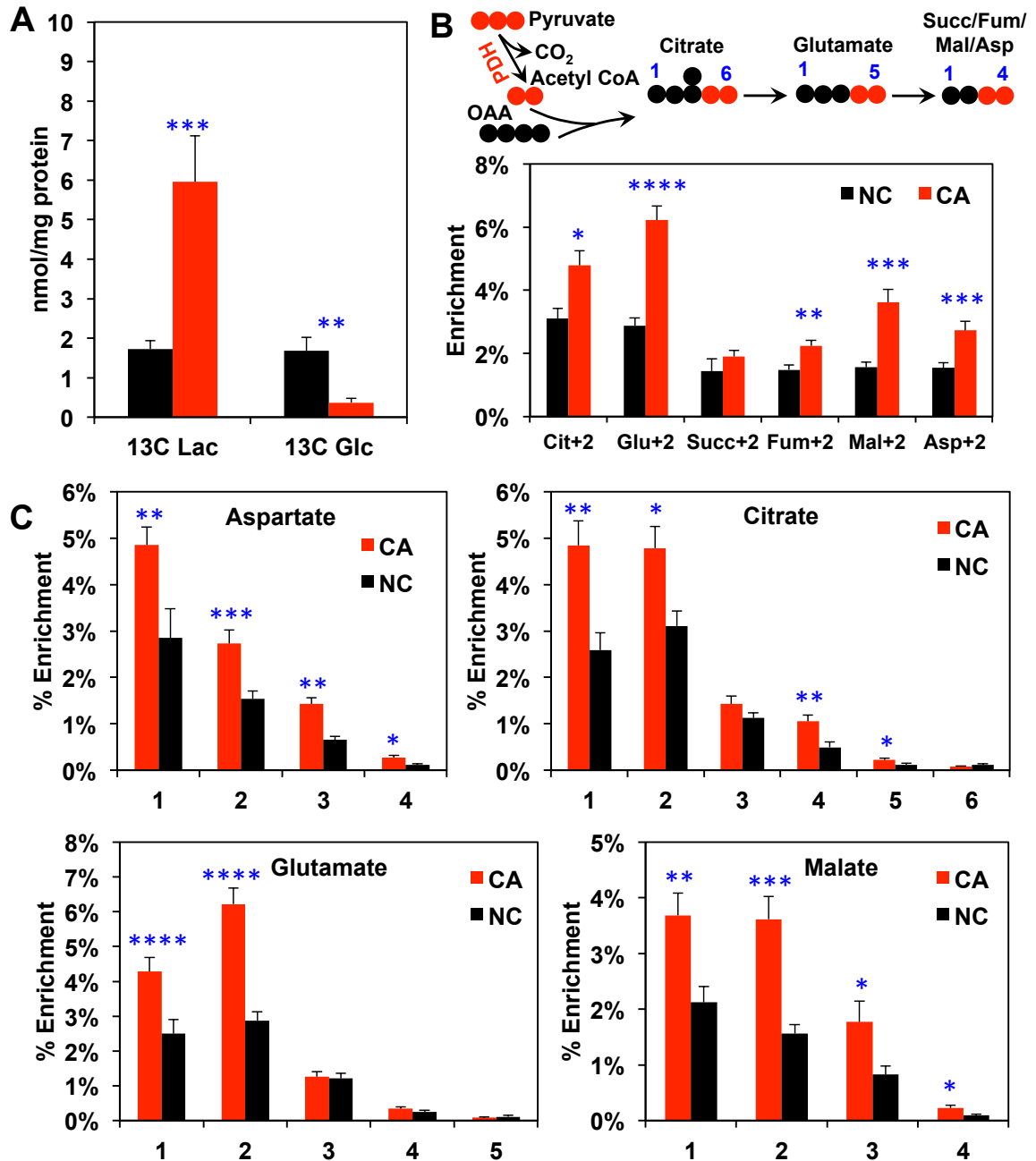


Figure S2: Glutamine oxidation via the Krebs cycle is not enhanced in ex vivo cancerous lung tissue slices compared to their paired non-cancerous counterparts.

A: At harvest, portions of the tissue slices were fixed in formalin and stained with hematoxylin and eosin. Pathological analysis confirmed that both tissue types exhibited normal histology after 24 hours of incubation, as illustrated for one pair. A: cancer cells; B: pneumocytes; C: macrophage.

B: 1D $^1\text{H}\{^{13}\text{C}\}$ HSQC analysis showed time course buildup of the ^{13}C abundance of glycolytic lactate (^{13}C -3-Lac) and Ala (^{13}C -3-Ala), and Krebs cycle metabolites Glu (^{13}C -3-Glu), succinate (^{13}C -2,3-suc), and Asp (^{13}C -3-Asp) in cancerous lung tissue slices treated with 10 mM $^{13}\text{C}_6$ -glucose for 0 (black), 3 (maroon), 9 (green), 24 h (orange lines), as described in Methods. The fresh tissue slices were obtained from the resected tumor of an NSCLC patient.

C: Thin slices of cancerous and non-cancerous lung tissues freshly resected from 13 human NSCLC patients were incubated with $^{13}\text{C}_5,^{15}\text{N}_2$ -glutamine for 24 hours (see Methods). The % enrichment of lactate, citrate, and glutamate was determined by GCMS. Cancerous and non-cancerous tissue

slices produced labeled glutamate (especially $^{13}\text{C}_5,^{15}\text{N}_1$ -glutamate or 6 isotopologue) after incubation with $^{13}\text{C}_5,^{15}\text{N}_2$ -glutamine, indicating active glutaminase.

However, except for Glu 5, there were no significant differences in the label pattern of glutamate or other Krebs cycle intermediates from incubation with labeled glutamine, suggesting that glutaminase is not more active in cancerous than in paired non-cancerous tissue slices. *: $p < 0.05$, **: $p < 0.01$ according to the Student t-test (N=13); Error bars represent standard error.

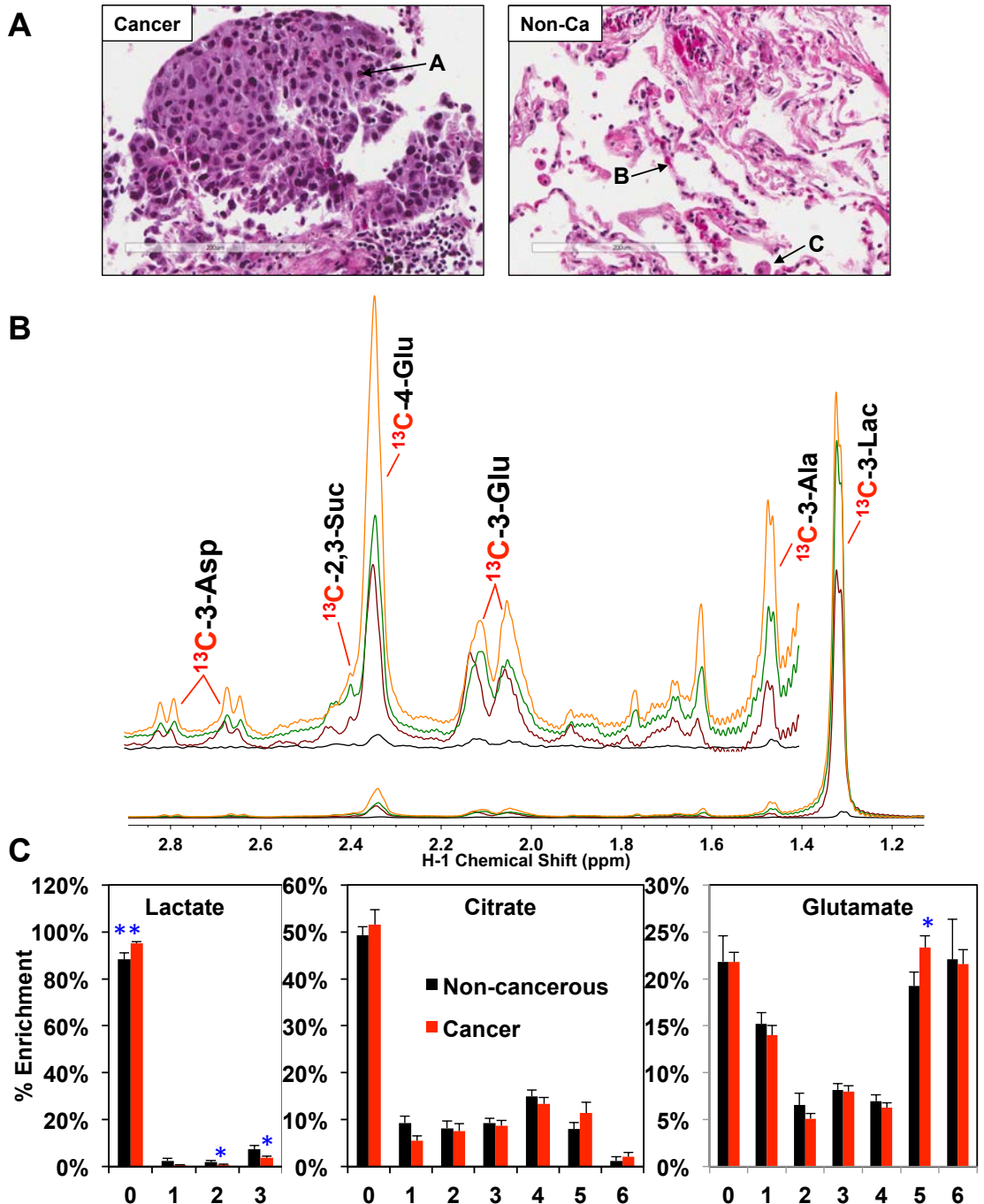


Figure S3: Immunohistochemistry shows preferential PC expression in malignant cells within NSCLC tumors

Pairs of cancerous and non-cancerous tissue sections obtained from NSCLC patients were stained with anti-PCB antibody, marking stain 3,3'-diaminobenzidine and counterstain hematoxylin.

A: Representative 4 pairs of tissue slides are shown. Viable cancer cells in the cancerous tissue (Cancer) stained intensely for PC while macrophages stained weakly and other stromal cells (fibroblasts and lymphocytes) showed no staining (left panels). In contrast, in the adjacent non-cancerous (Non-Ca) tissue, macrophages stained strongly for PC while pneumocytes and other stromal cells (smooth muscle cells, endothelial cells, pneumocytes, and red blood cells) stained very weakly (right panels). In addition, abnormal atypical adenomatous hyperplasia (AAH) was detected in the Non-Ca tissue and stained heavily with PC (top two right panels).

B: PC staining was semi-quantified using a thresholding method to determine the number of DAB-positive pixels in a 1232 by 715 pixel image. Cancerous tissues had more PC-positive pixel than their non-cancerous pairs. Five images taken from different regions of each tissue were averaged and error bars represent standard errors. *: $p < 0.05$, **: $p < 0.01$, ***: $p < 0.001$, based on the Student t-test assuming unequal variances; Error bars represent standard error (N=4).

C: A549 cells were co-stained with nuclear stain DAPI (blue), mito-tracker red and a PC antibody (green). The merged images show that PC co-localizes with the mitochondria, which cluster around the nuclei (blue).

D: High magnification IHC images of cancerous lung tissues show also perinuclear localization of PC.

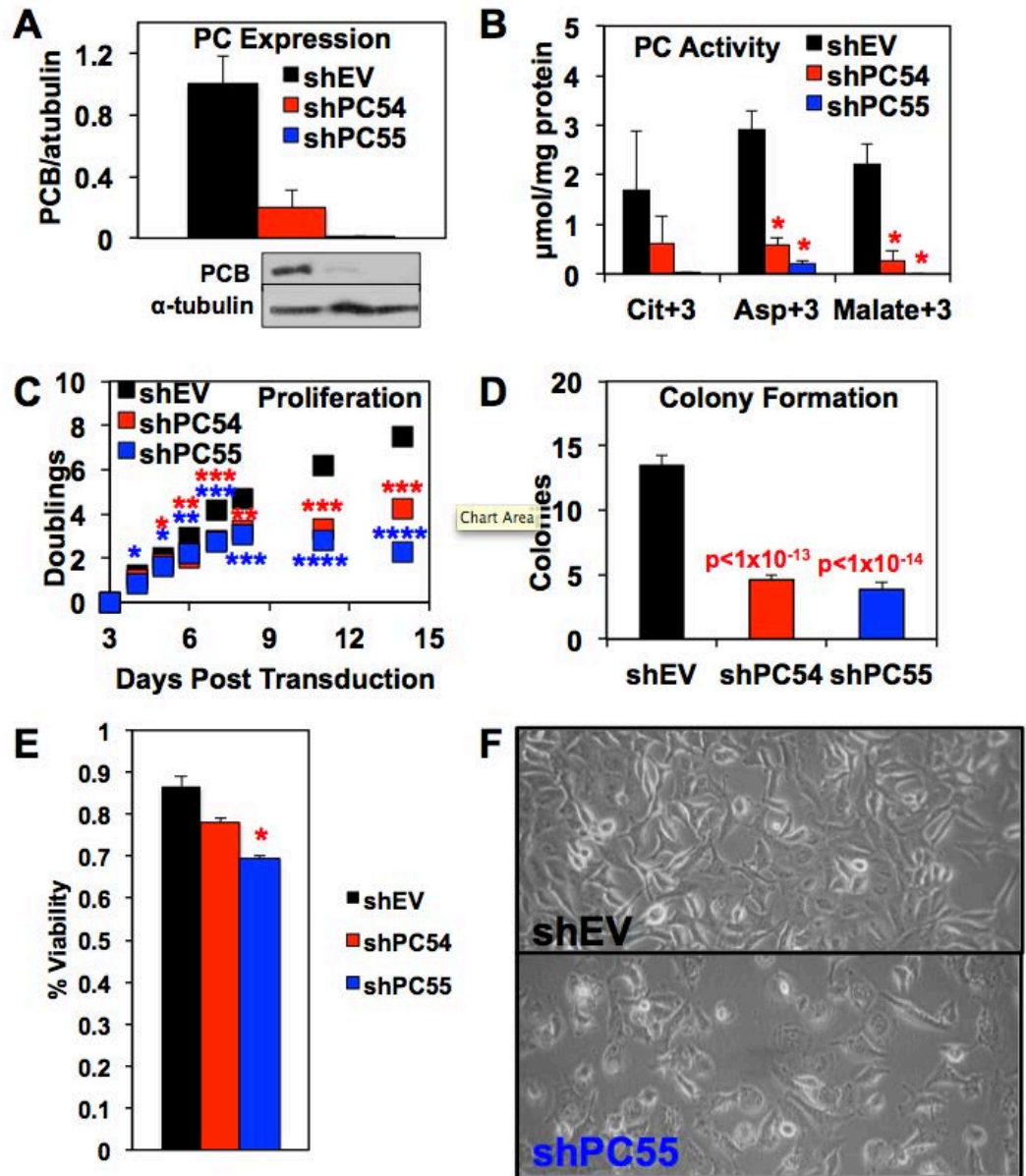


Figure S4: PC suppression inhibits proliferation and tumorigenicity of human adenocarcinoma A549 cells

A: A549 cells were transduced with two shRNAs targeting PC (shPC54 and shPC55) and a control shRNA containing an empty vector (shEV). Western blots showed PC levels were reduced by 80% (shPC54) and ~99% (shPC55) five days after transduction with shRNA in duplicate cell cultures (N=2).

B: In cell PC activity, assayed by the metabolism of $^{13}\text{C}_6$ -glucose to $^{13}\text{C}_3$ -citrate, $^{13}\text{C}_3$ -aspartate, and $^{13}\text{C}_3$ -malate (Cit+3, Asp+3, and Malate+3, respectively) showed a large decrease in PC knockdown cells. shPC55 inhibition was greater than shPC54. The assay was performed in triplicate (N=3) 8 days post-transduction. The concentration of ^{13}C isotopologues was determined by GCMS. Error bars represent standard error.

C: Triplicate cell growth assay, initiated 3 days post transduction, revealed a substantial time-dependent decrease in cell doubling by shRNA-transduced cells: shPC55 inhibition was greater than in shPC54-transduced cells. There was a relatively long latency period (>6 days) before cell growth was compromised.

D: Colony formation assay was initiated 2 days post transduction and assessed 14 days later. PC knockdown cells have a greatly reduced capacity to form colonies in soft agar. Each value is the average of 20 fields of view, and averaged over duplicate cell cultures (N=20).

E: Viability assessment by Trypan blue staining 8 days post-transduction. shPC55 reduced viability by 15% at this time point. Triplicate cultures; error bars represent standard error.

F: Micrographs show the morphology of control shEV A549 cells and A549 cells 8 days post PC knockdown by shPC55.

Values represent the averages. *: $p < 0.05$, **: $p < 0.01$, ***: $p < 0.001$, ****: $p < 0.0001$ based on the Student t-test assuming unequal variances; Error bars represent standard error.

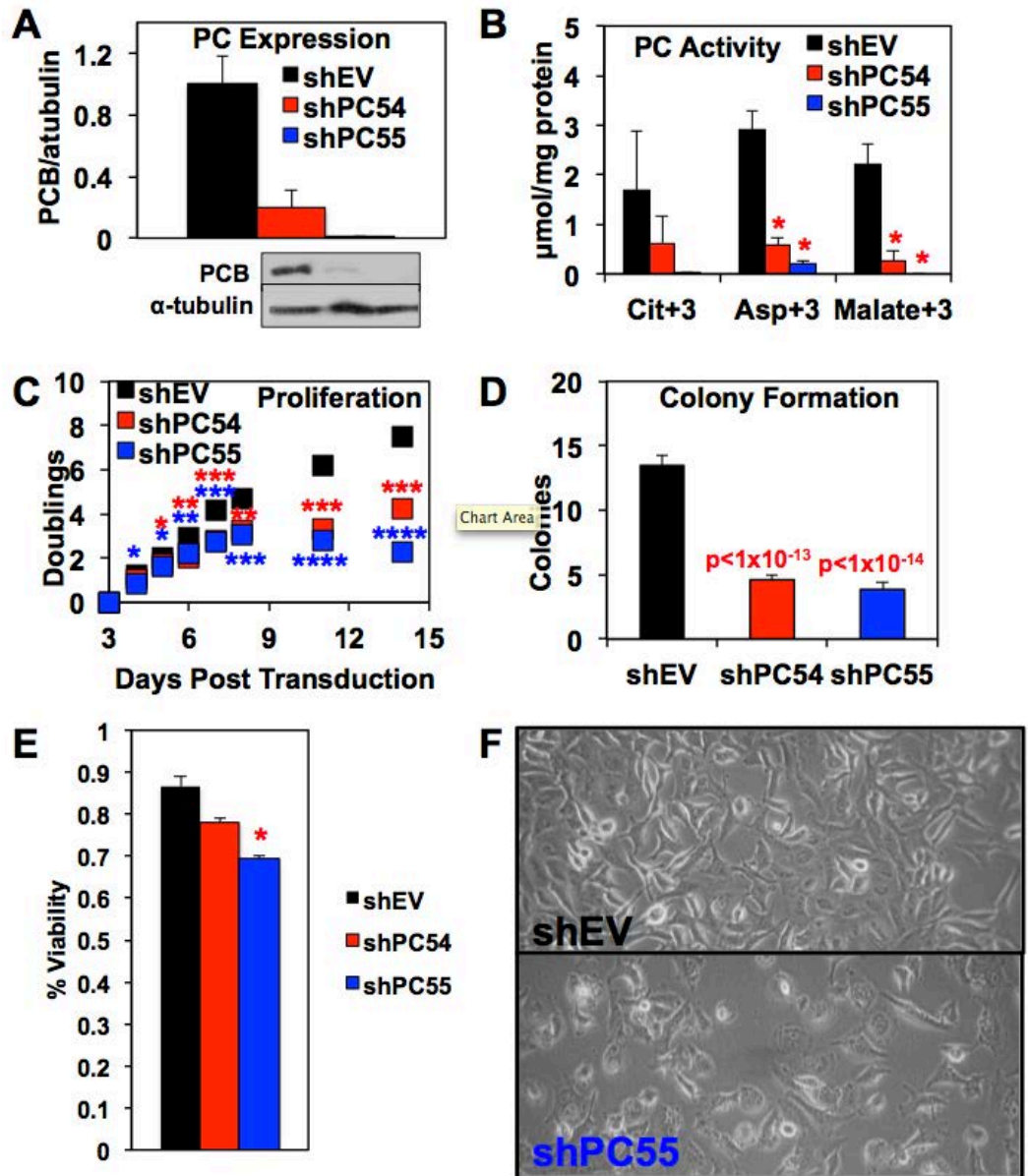


Figure S5: The shPC55 construct effectively suppressed PC expression in 5 NSCLC cells lines and in A549 mouse xenografts, as well as inhibited tumorigenicity in 3 cell lines.

A: Western blot analysis of A549, H1299, H2030, HCC827, and PC9 NSCLC adenocarcinoma cells transduced with shPC55 showed reduced PC expression by the vector to nearly undetectable levels in all 5 cell lines. In addition, control (shEV) cell lines bearing an EGFR mutation (HCC827 and PC9) had higher PC expression than those with a KRAS or NRAS mutation (A549 and H1299) with the exception of H2030.

B: A549, H1299, and PC9 cells transduced with shPC55 or shEV before seeding in soft agar, as described in Methods. After sufficient time for colony formation, cells were stained with crystal violet. As shown in the representative well images, shEV-transduced cells formed more and larger colonies than shPC55-transduced cells. The number of colonies were counted in triplicate cultures and the enumerations are provided in **Figure 4D**.

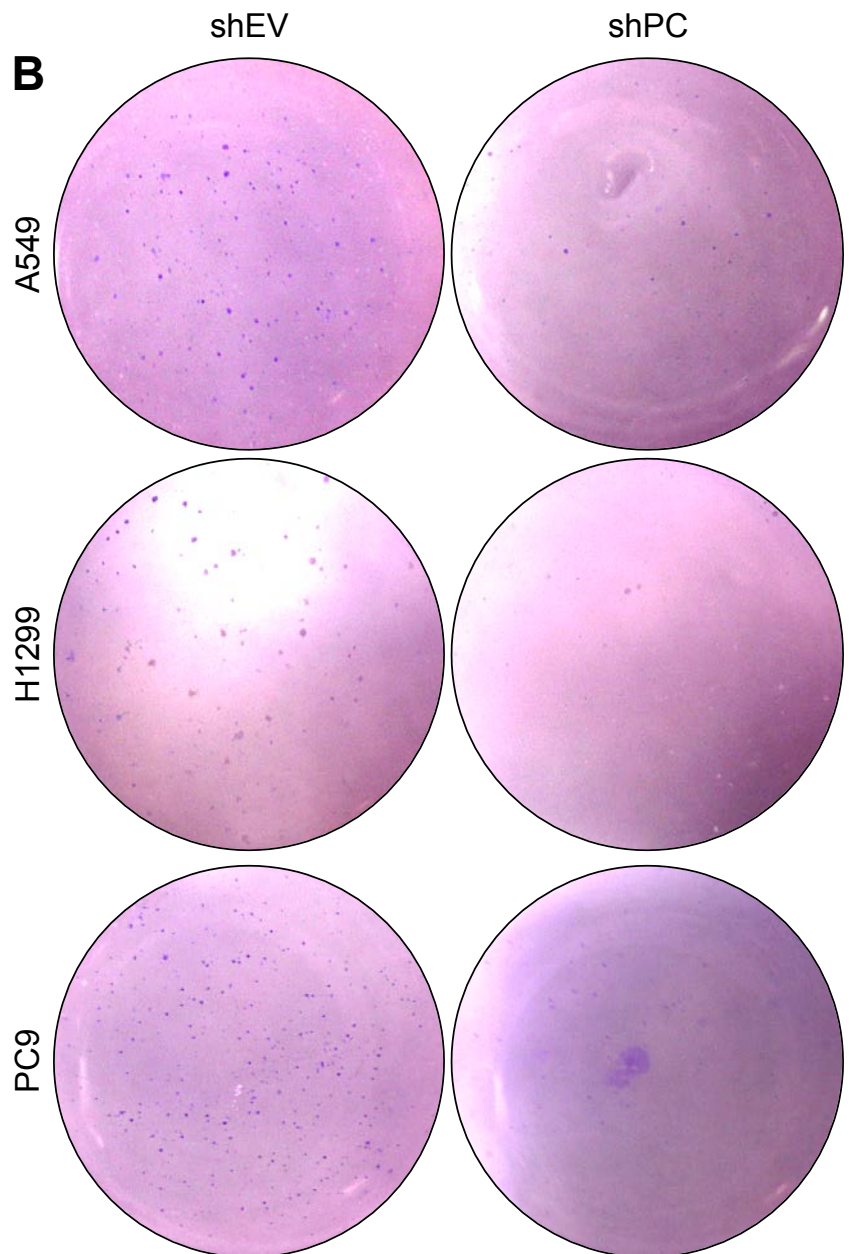
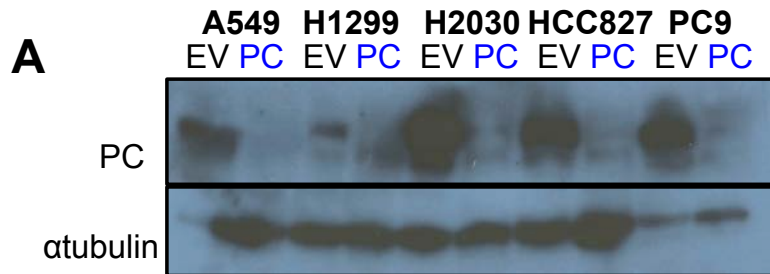
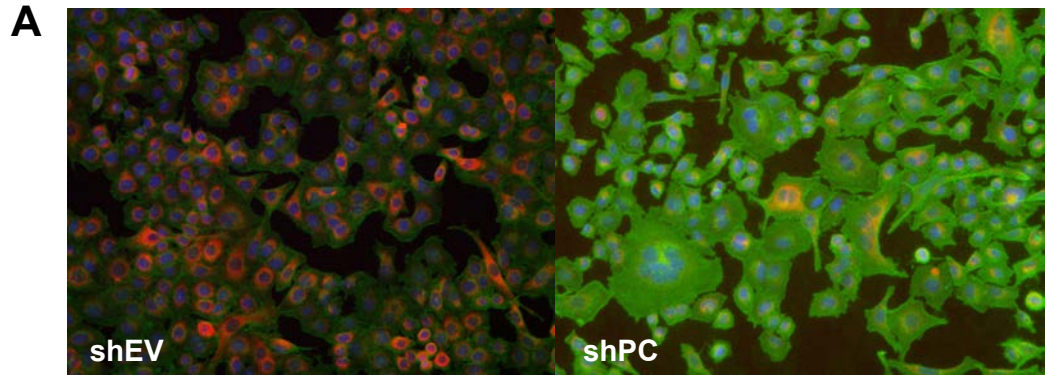
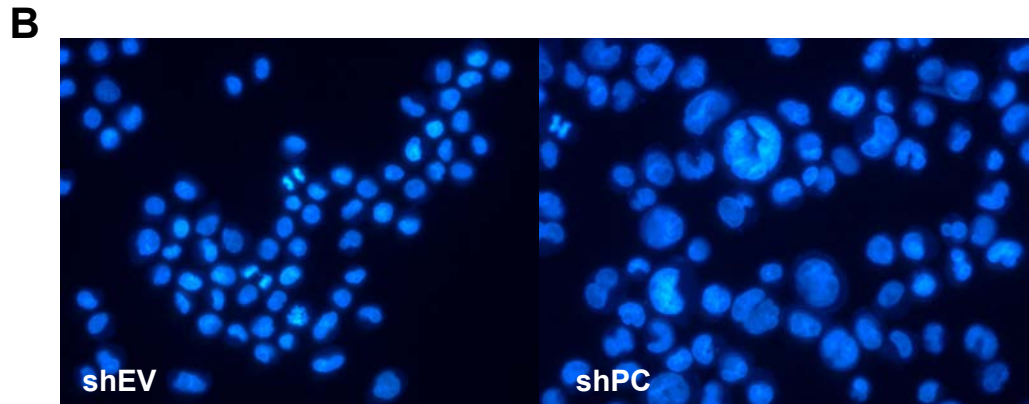


Figure S6: Fluorescence microscopy reveals that PC knockdown reduces mitochondrial membrane potential and induces multinucleation

A: A549 cells were seeded on coverslips in 6-well plates. After 48 hours, cells were fixed in 4% paraformaldehyde and permeabilized with 0.1% Triton X-100. Nuclei (blue) and actin filaments (green) were stained respectively with Hoechst 33342 and Alexa 488 conjugated to phalloidin. Mitochondrial membrane potential was assessed by staining the live cells with Mitotracker Red CMXRos (red). Micrographs reveal that PC knockdown cells were larger, accumulated multiple nuclei, and had lower mitochondrial membrane potential and/or fewer mitochondria.



B: Nuclear morphology was assessed by staining with Hoechst 33342 (blue). PC knockdown A549 cells contained multiple distinct nuclei at Day 8 post-transduction.



C: shEV or shPC55-transduced A549 cells (200) with distinct nuclear morphologies were counted at Day 8 and 12 post transduction. PC knockdown cells had fewer normal nuclei than control cells and the degree of multinucleation increased over time.

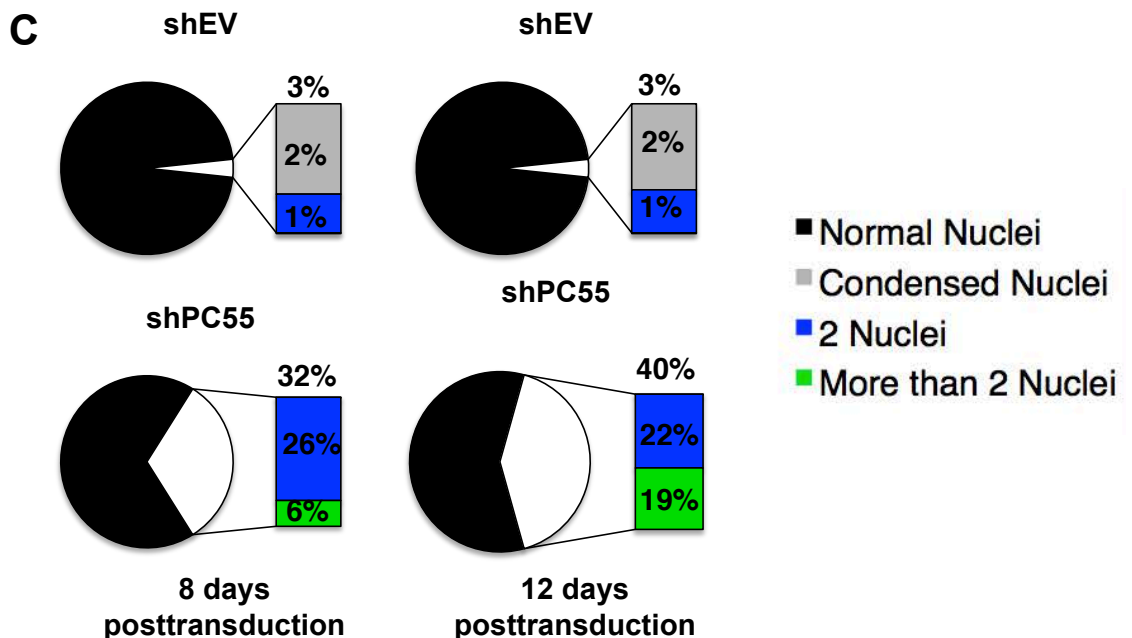


Figure S7: PC knockdown does not affect aerobic glycolysis in A549 cells *in situ* or *in vivo*

A: Western blot analysis of mouse tumor xenografts derived from shPC55- or shEV-transduced A549 cells confirms PC suppression in the shPC tumors; however, the severity of the knockdown was less than that in cell cultures (cf. Fig. S5A). shPC tumors had on average 30-60% the PC expression of shEV tumors.

B: A549 cells were transduced with shPC55 or shEV. Proton NMR analysis of media from triplicate cultures incubated in $^{13}\text{C}_6$ -glucose for 24 hours revealed that PC knockdown did not affect glucose consumption, total lactate production (Lactate) or ^{13}C -lactate derived from labeled glucose.

C: GCMS analysis of the same cell media shows that the %enrichment of labeled lactate derived from $^{13}\text{C}_6$ -glucose was similar between shEV and shPC cells. 0-3 refer to $^{13}\text{C}_{0-3}$ -lactate isotopologues.

D: A549 cells transduced with shPC55 or shEV were engrafted into NSG mice and treated with $^{13}\text{C}_6$ -glucose as described in Methods. Proton NMR analysis of the tumor tissues show that total lactate and labeled lactate derived from the glucose tracer was not affected by PC knockdown (N=5-6 for each tumor type).

E: GCMS analysis of the same tissues confirms that % ^{13}C lactate enrichment was similar between shEV and shPC tumors, corroborating the results from cell culture. N=5 or 6 mice.

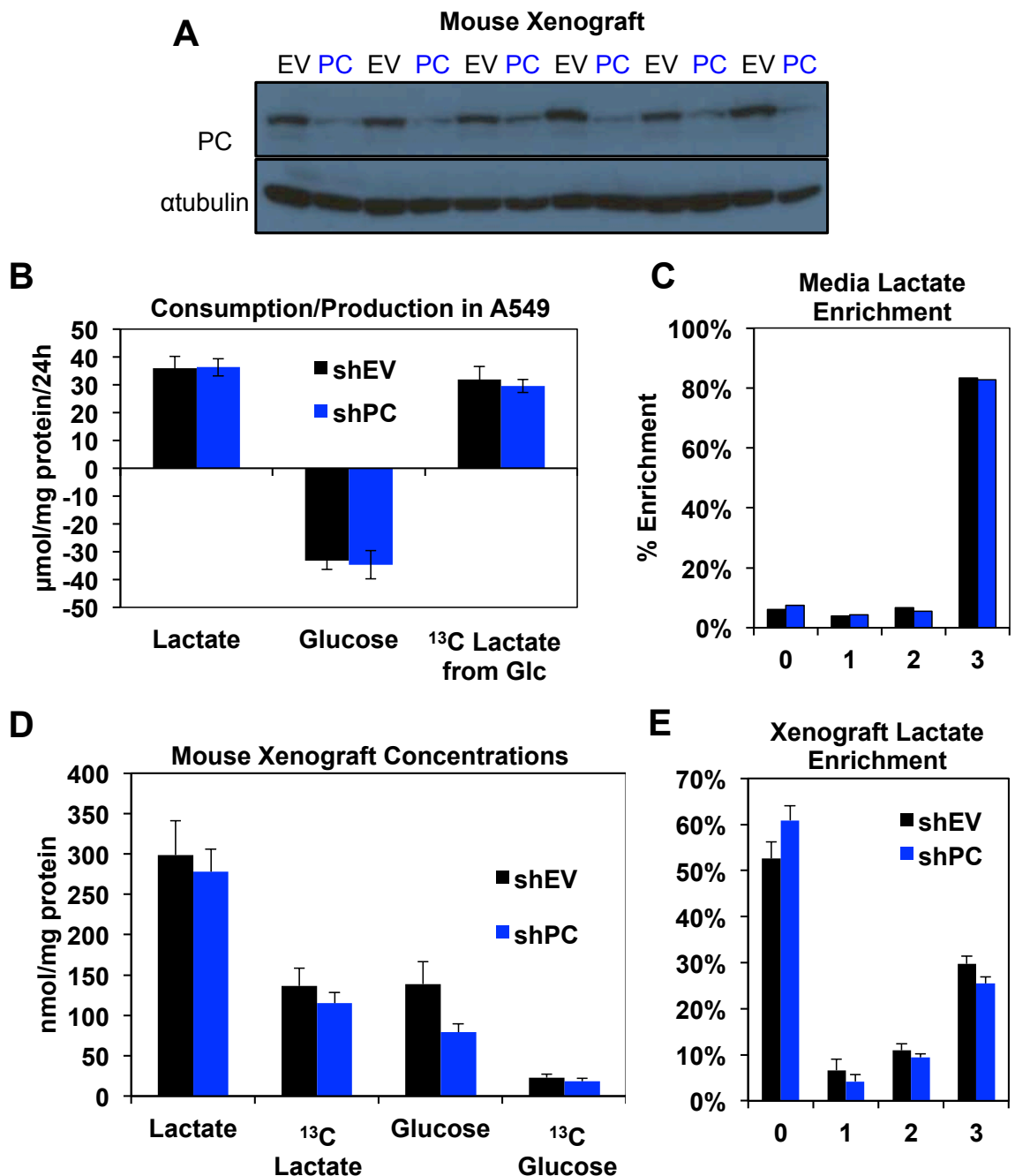


Figure S8: Mouse xenografts with PC-suppressed cells have reduced glucose oxidation through the Krebs cycle

The same mouse xenograft tumor extracts from **Fig. S7C** (N=6) were analyzed by GCMS for the level and % enrichment in the ^{13}C isotopologues of citrate, glutamate, succinate, and aspartate. Tumor bearing the PC knockout vector had reduced level and/or enrichment of the Krebs cycle activity markers $^{13}\text{C}_2\text{-Asp}$ (2) or $^{13}\text{C}_3\text{-Asp}$, succinate (3) and $^{13}\text{C}_5\text{-citrate}$ (5), which indicate decreased glucose entry via pyruvate dehydrogenase or pyruvate carboxylase, respectively. Values represent the averages of 5 control and 6 PC-knockdown replicates. *: $p < 0.1$, **: $p < 0.05$, ***: $p < 0.01$, based on the Student t-test assuming unequal variances; Error bars represent standard error.

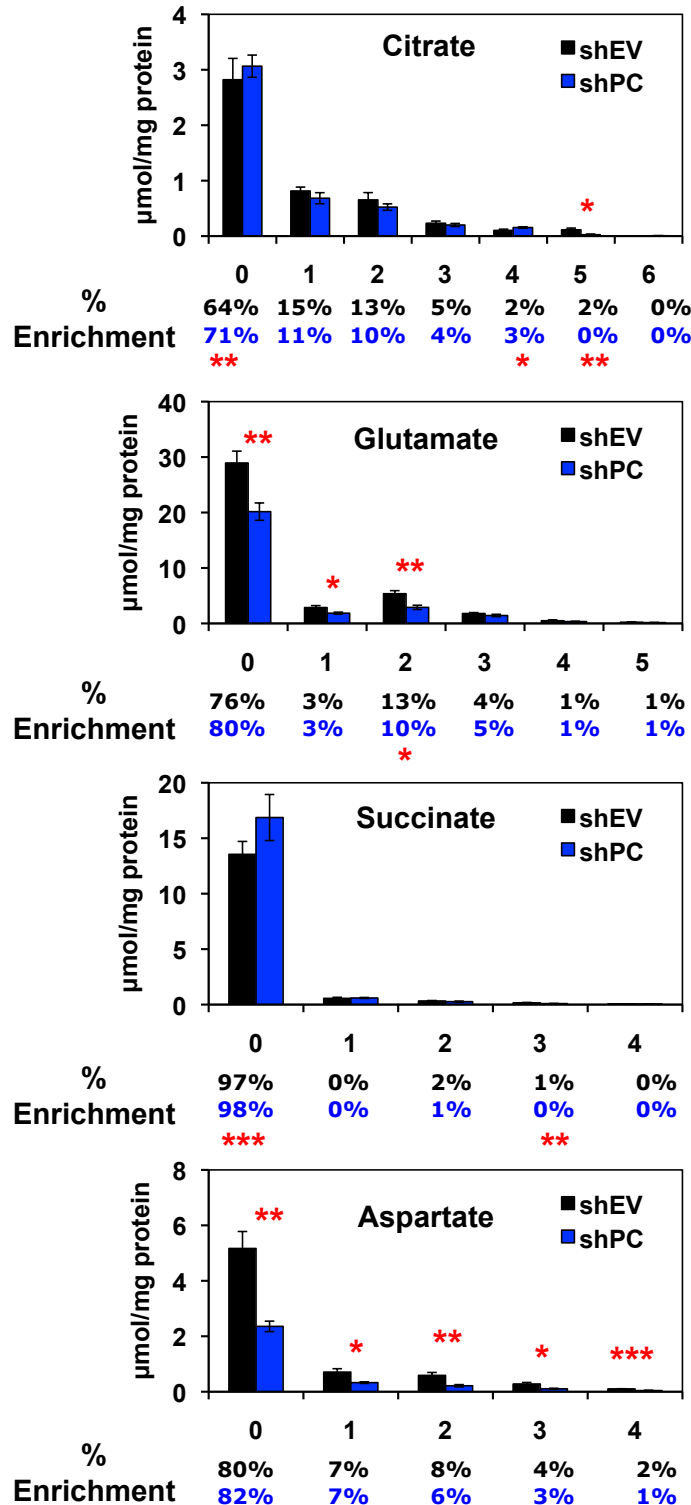


Figure S9: $^1\text{H}\{^{13}\text{C}\}$ HSQC analysis of PC knockdown cell and mouse tumor extracts reveals perturbed glucose and glutamine metabolism

A549 cell transduction, xenografting, and tracer treatment are described in Methods.

A and B: shPC55 and shEV-transduced cells were incubated with $^{13}\text{C}_6$ -glucose (**Panel A**) or $^{13}\text{C}_5,^{15}\text{N}_2$ -glutamine (**Panel B**) for 24 h. Experiments were performed in triplicate in two separate experiments. Shown are the representative spectra from one experiment. Asterisks represent peaks with significantly different intensities between PC knockdown and control cells. PC suppressed cells had less glucose carbon incorporated into Krebs cycle metabolites (e.g. citrate, Asp, Glu, glutathiones) and the ribose moiety of nucleotides. Likewise, PC knockdown cells displayed reduced glutamine carbon incorporation into glutamate, Asp, and glutathione. Lac: lactate; GSH: reduced glutathione; GSSG: glutathione disulfides; Cit: citrate.

C: The cells from above were xenografted into mice, which were then treated with $^{13}\text{C}_6$ -glucose. $^1\text{H}\{^{13}\text{C}\}$ HSQC spectra of the resulting tumors show many of the same metabolic perturbations as the cell culture experiment but without reaching statistical significance. The latter could be attributed to the less effective PC suppression in tumor xenografts than in cell cultures. Glc: glucose.

Significance was determined by quantifying metabolite concentrations in triplicate cultures. *: $p < 0.05$, **: $p < 0.01$, ***: $p < 0.001$, based on the Student t-test assuming unequal variances.

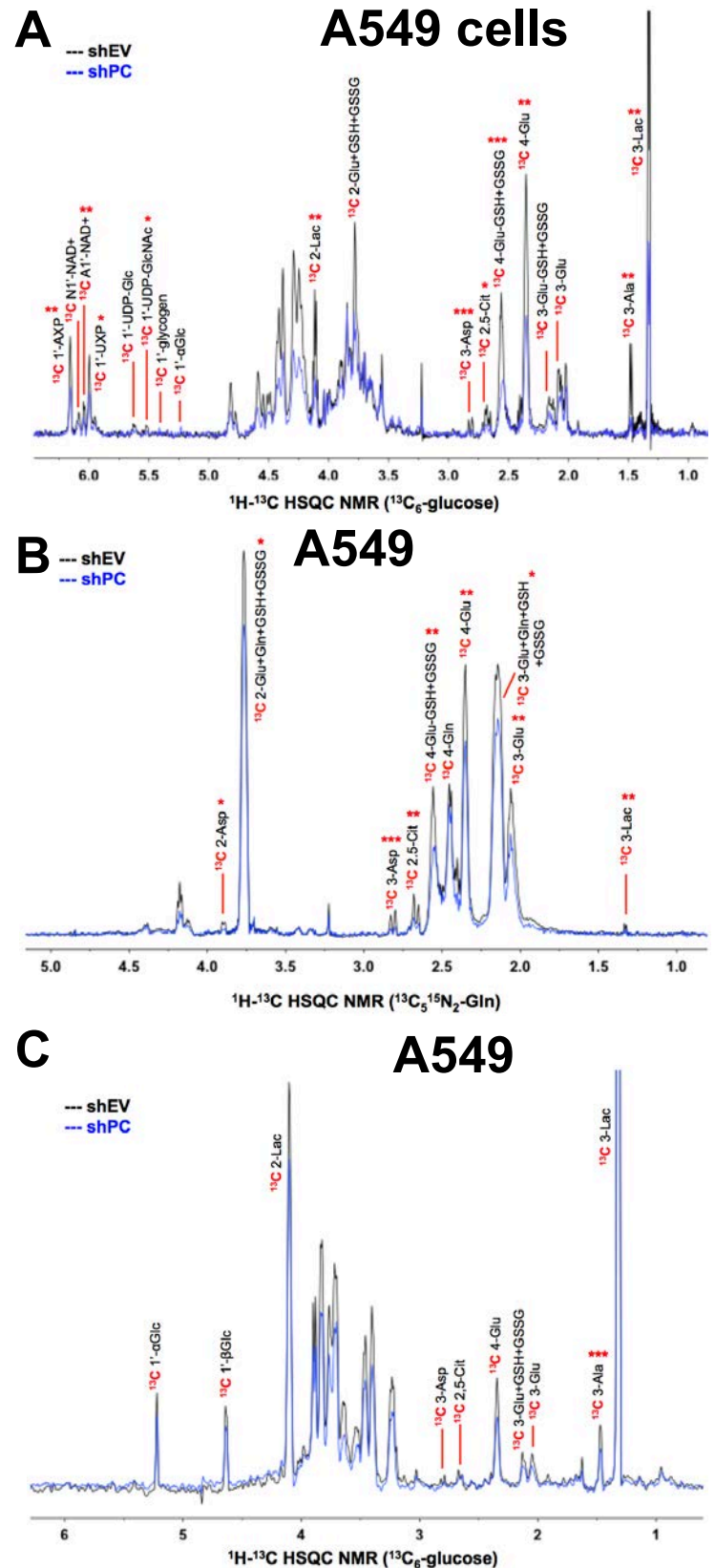


Figure S10: Glutamine metabolism via GLS1 does not compensate for lost PC expression *in cells* or *in vivo*

A: Left panel: GLS1 protein expression was reduced in PC knockdown A549 cells. Right panel: tumors derived from shPC-bearing A549 cells had on average 40% less glutaminase 1 (GLS1) expression than those derived from shEV-bearing cells, based on Western blot analysis ($p > 0.005$, based on the Student t-test assuming unequal variances).

B: A549 cells were transduced with shPC55 or shEV for 3 days and then grown in 2 or 0.2 mM glutamine. Cell density was measured daily by the Janus Green assay in at least triplicate cultures, as described in Methods. Glutamine restriction reduced the number of control (shEV) cells by 3 fold over the course of 4 days but had little effect on the growth of PC knockdown cells.

C: The log base 2 of the normalized cell density at each day (relative to initial cell density) from **B** was plotted against day and the linear regression of the plot was used to estimate the doublings per day as growth rate. The growth rates of shEV cells were significantly reduced by glutamine restriction (2 mM versus 0.2 mM). While the growth rate of PC knockdown cells was significantly lower than that of shEV cells at each glutamine concentration, there was no additional negative affect of glutamine restriction on shPC cell growth. *: $p < 0.05$, **: $p < 0.01$, ***: $p < 0.001$, based on the Student t-test assuming unequal variances; Error bars represent standard error of triplicates.

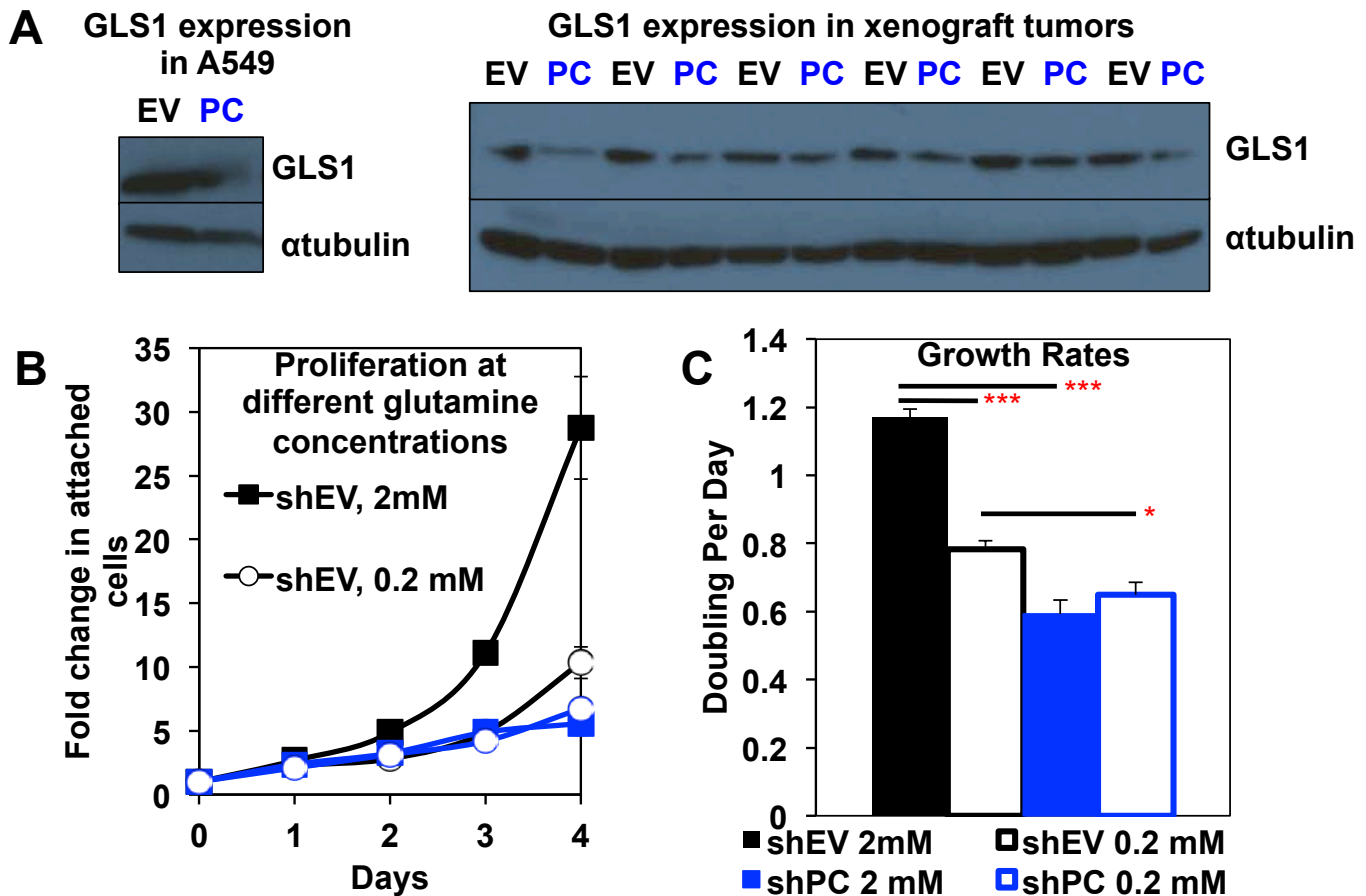


Figure S11: PC knockdown reduces nucleotide levels and purine biosynthesis

A: A549 cells were transduced with shPC55 or shEV, as described in Methods. PC knockdown cells had lower concentrations of uracil and adenine-containing nucleotides (UXP and AXP, respectively), as measured by ^1H NMR. In addition, when the cells were incubated in $^{13}\text{C}_6$ -glucose for 24 hours, PC knockdown cells incorporated less ^{13}C into the ribose subunit of AXP (^{13}C 1'AXP) and the ribose unit attached to the adenine ring of NAD^+ (^{13}C A1' NAD^+), as measured by $^1\text{H}\{^{13}\text{C}\}$ HSQC NMR (cf. **Fig. S9A**). Each value represents an average of triplicates.

B: A similar depletion in uracil and adenine-containing nucleotides was evident in mouse tumor xenografts derived from shPC55-transduced A549 cells relative to those transduced with shEV. Each value represents an average of six replicates.

*: $p < 0.05$, **: $p < 0.01$, ***: $p < 0.001$, based on the Student t-test assuming unequal variances; Error bars represent standard error.

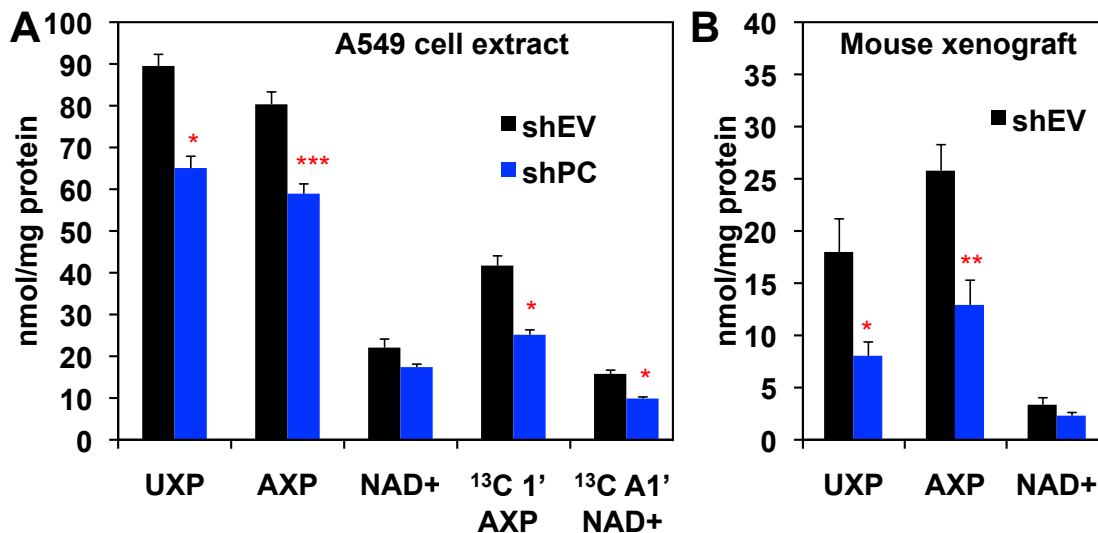


Figure S12: PC knockdown perturbs glutathione homeostasis and increases ROS production and sensitivity

A-C: ^1H NMR (**A,C**) and $^{13}\text{C}\{^1\text{H}\}$ HSQC NMR analysis (**B**) of shPC55- and shEV-transduced A549 cells showed that PC knockdown depleted reduced glutathione (GSH) while increasing levels of oxidized glutathione (GSSG), leading to significantly lowered GSH:GSSG ratio (**C**). These changes are related to reduced *de novo* synthesis of glutathiones from ^{13}C -glucose or ^{13}C -glutamine (**B**). The reduced GSH:GSSG ratio was also observed in mouse tumor xenografts of shPC55-transduced A549 cells (**C**). Cell experiments were performed in triplicate and the mouse xenograft experiment was performed with six replicates.

D: PC knockdown cells had greater levels of intrinsic ROS, as detected by DCFDA

fluorescence (0 mM H_2O_2 data). When cells were treated with increasing concentrations of H_2O_2 , PC-suppressed cells were much less able to quench ROS. Each condition represents an average of six replicates.
 *: $p < 0.05$, **: $p < 0.01$, ***: $p < 0.001$, ****: $p < 0.0001$, based on the Student t-test assuming unequal variances; Error bars represent standard error.

E: A549 cells were treated with 10 mM N-acetylcysteine (NAC) prior to transduction with shPC55 to determine if ROS production contributed to attenuated proliferation by PC knockdown. Growth assays showed little rescue with NAC treatment in PC-knockdown cells. Each value represents the average of three replicates.

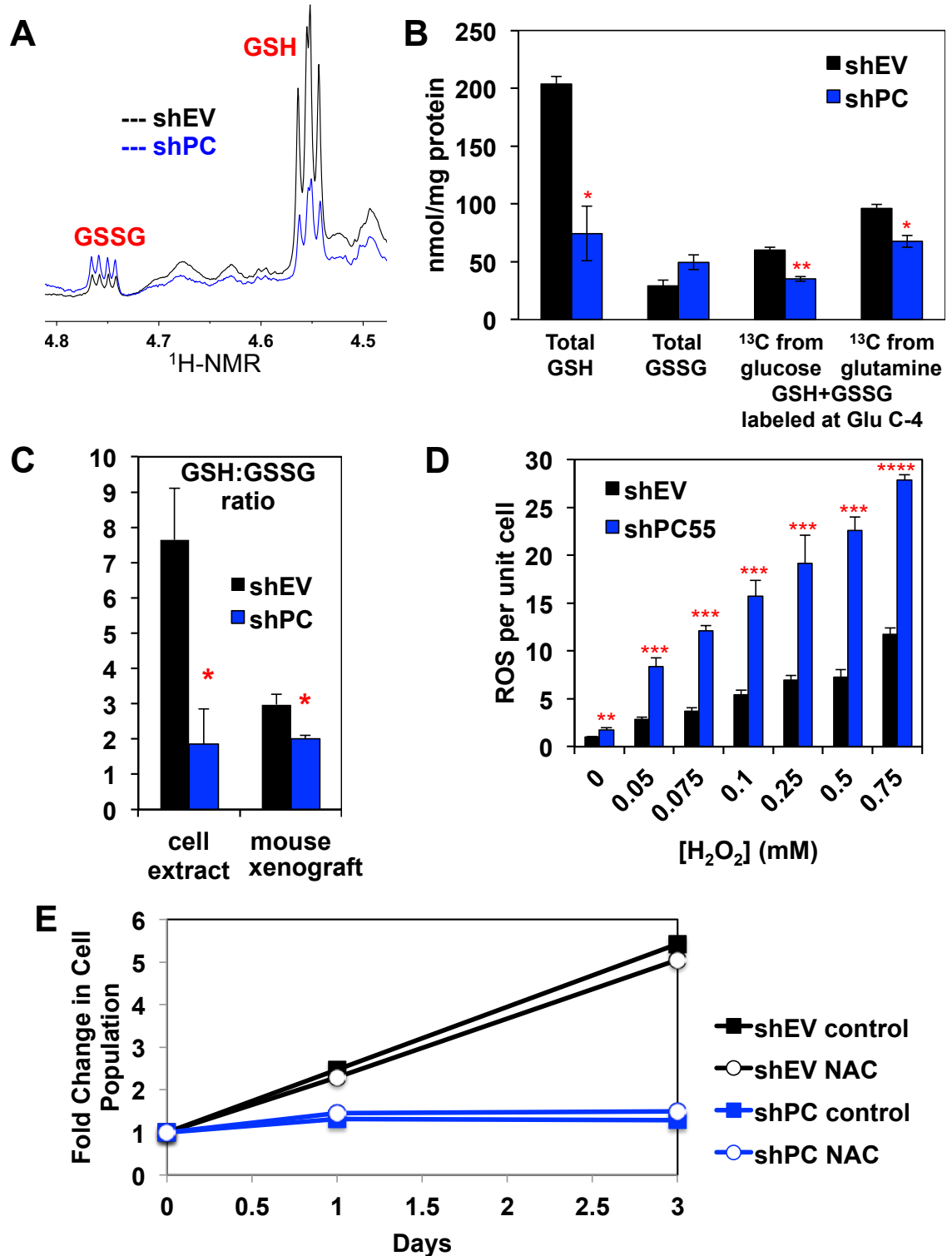


Figure S13: Growth inhibition and multiple metabolic perturbations are observed in A549 cells transduced with shPC55 relative to those transduced with a scrambled shRNA

A549 cells were transduced with shPC55 or shScr (scrambled) vector for 2 days before selection in 1 $\mu\text{g/ml}$ puromycin. The shScr sequence used was 5'-CCGGCCTAAGGTTAAGTCGCCCTCGCTCGAGCGAGGGCGACTTAACCTTAGGTTTTTG -3'. The cells were then seeded for proliferation and $^{13}\text{C}_6$ -glucose tracer experiments, as described in Supplemental Methods and Methods, respectively. As shown in panel **A**, the growth of shPC55-transduced cells was greatly inhibited relative to that of shScr-transduced cells, as in the case of shPC55- versus shEV-transduced cells (cf. **Fig. 4A**). Likewise, multiple metabolic perturbations were evident in shPC55- versus shScr-transduced cells. In addition to reduced synthesis of e.g. $^{13}\text{C}_3$ -Asp (data not shown), which reflects reduced PC activity, the production of many other metabolites was also inhibited, such as ^{13}C labeled Ala (**B**), AXP/ATP (**B,C**), UXP (**B**), CTP (**C**), total glutathiones (GSH/GSSG) (**B**), phosphatidylcholines (PCh), and triacylglycerides (TAG) (**D**). The similar set of metabolic changes observed here as those observed in **Figs. 6** and **S12B** support the specific role of PC in eliciting these perturbations, instead of being a general effect of shRNA. Data in **B** and **C,D** were obtained from 1D HSQC and FT-ICR-MS analysis, respectively. Each value in **A** and **B-D** was respectively an average of 5 and 3 replicates with error bars representing SEM. * $p < 0.01$, ** $p < 0.005$, *** $p \leq 0.001$, **** $p \leq 0.0001$, ***** $p \leq 0.0005$, ***** $p \leq 0.00001$, ***** $p < 5 \times 10^{-6}$, ***** $p < 5 \times 10^{-7}$, ***** $p < 2 \times 10^{-8}$, from paired Student t-test assuming unequal variances; Error bars represent standard error.

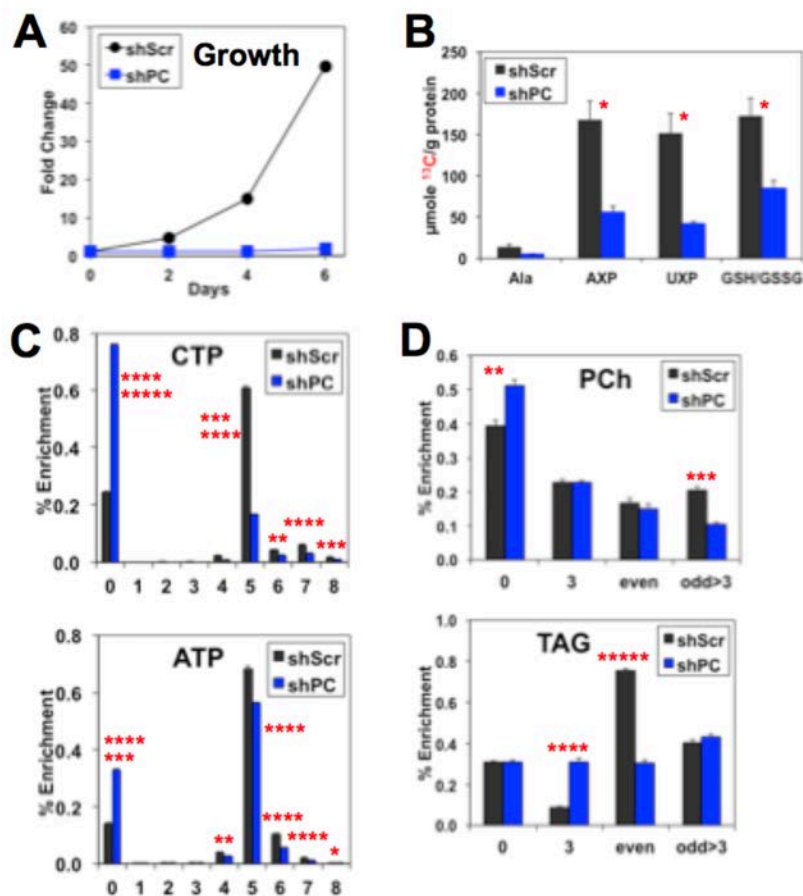


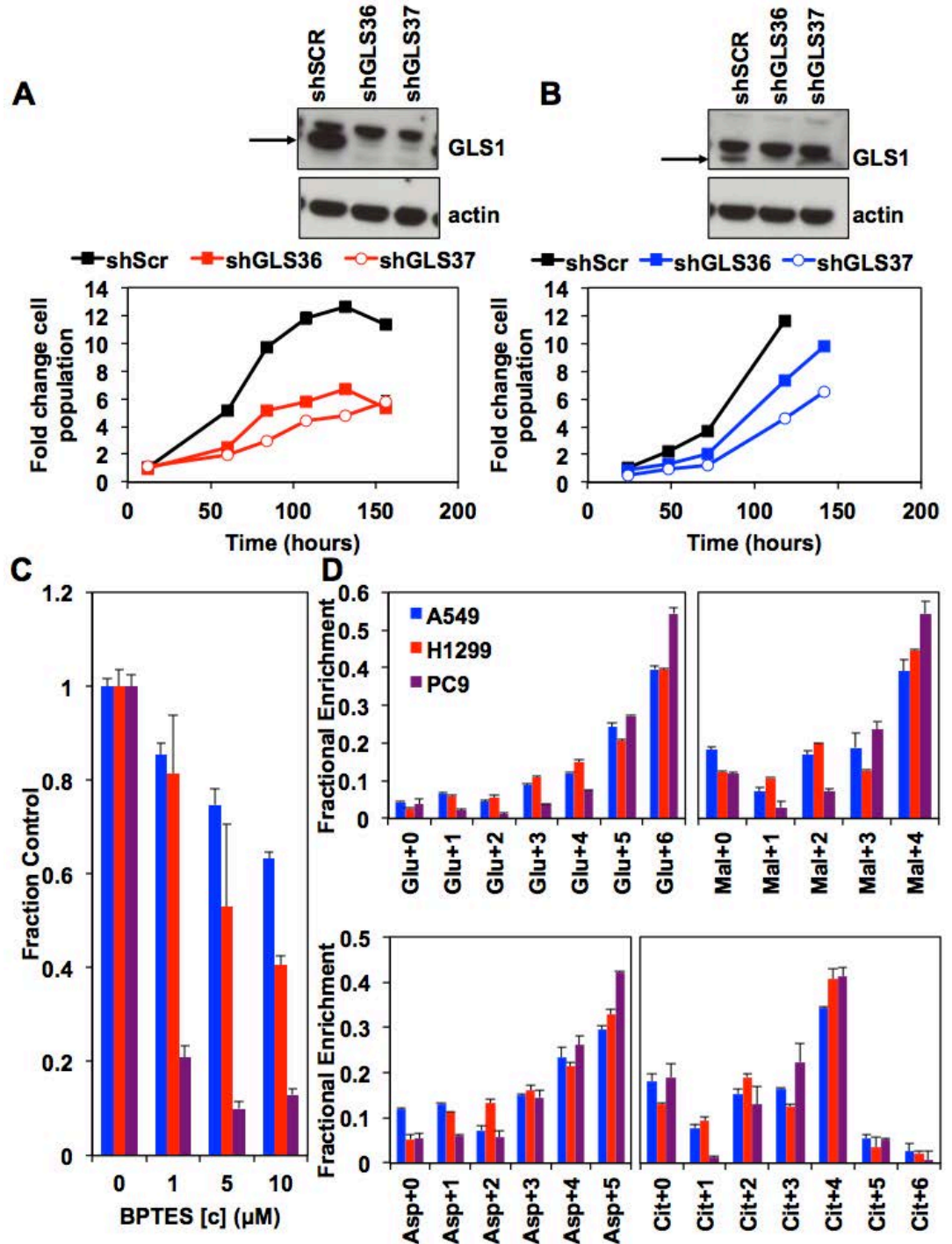
Figure S14: NSCLC cells also require glutaminase and use glutamine as a source of anaplerosis

A-B: A549 (A) and H1299 (B) cells (from ATCC) were transduced with a scrambled vector and two shRNA vectors specific for glutaminase 1 (GLS1). GLS1 knockdown by either vector significantly reduced the growth rate in H1299 cells ($p < 0.02$; Welch test on specific growth rate obtained by non-linear regression and comparison with the scrambled vector, cf. Fig. 4), but not for A549 ($p \approx 0.5$). For A549, the death rate was higher in cells transduced with GLS shRNAs.

C: The growth of these cells lines were also sensitive to GLS1 inhibitor bis-2-(5-phenylacetamido-1,2,4-thiadiazol-2-yl)ethyl sulfide (BPTES). Each value represent the average of triplicate cultures and error bars represent standard error. P values by Student t-test for 5 and 10 μM BPTES were 0.007, 1E-7 for A549 (blue); 2E-15, 8E-16 for PC9 (red); H1299 (purple) 0.04, 6E-12.

D: To determine whether these NSCLC cells lines use glutamine carbon as a source of anaplerosis, A549, H1299, and PC9 cells were incubated with $^{13}\text{C}_5, ^{15}\text{N}_2$ -glutamine for 24 hours. Incorporation of glutamine carbon into the Krebs cycle metabolites was determined by GCMS. In every case, these metabolites were highly enriched in ^{13}C , suggesting glutamine as a significant source of anaplerosis in these cells.

Each condition



represents an average of three replicates. Error bars represent standard error.